Investigation of Pc5 pulsations effects and magnetospheric processes during intense geomagnetic storms

Sarup Khadka Saurav Saurav[1], Monika Karki[2], Binod Adhikari[3], Ashok Silwal[4], Luciano Aparecido Magrini[5], Ezequiel Echer[6], Odim Mendes[6], Margarete Oliveira Domingues[6], and Sujan Prasad Gautam[7]

[1]Patan Multiple college, Tribhuvan University
[2]Amrit Campus, Tribhuvan University
[3]St.Xavier's College, ,Maitighar
[4]Patan Multiple Campus, Tribhuvan University
[5]1Federal Institute of Education, Science and Technology of São Paulo (IFSP),
[6]National Institute for Space Research (INPE)
[7]Central Department of Physics, Tribhuvan University

November 23, 2022

Abstract

Giant pulsations belonging to the Pc5 frequency band were conceived by Rolf (1931). Such pulsations are influenced by magnetospheric processes produced by the solar wind. The purpose of this study is to investigate the Pc5 ULF waves and their relationship to solar parameters and geomagnetic indices, respectively, utilizing data from ground-based magnetometers and data provided by Operating Mission as Nodes on the Internet (OMNI). Magnetic observatories over Earth's surface reported intense long-period ULF activity on 19 28 February 2014 and 22-23 June 2015. We discovered a highly significant correlation between global Pc5 ULF waves and other interplanetary parameters, as well as a clear peak-to-peak correspondence during storms. We performed continuous wavelet transform (CWT) on the Pc5 integrated power (Ipow) and discovered that the majority of the intense Pc5 spectra are localized within the 64-256 minute Fourier period band. Our results suggest that geomagnetic fluctuations observed at low latitudes do not originate locally but rather are a reflection of global geomagnetic field variations with primary sources in the magnetosphere and high latitude ionosphere, which is consistent with the study of Gupta (1976). We discovered only nominal effects of IMF Bz on Pc5 pulsations, despite its southern counterpart being widely believed to be the principal driver of geomagnetic storms. Additionally, we discovered a moderate effect of solar wind pressure on Pc5 pulsations. A cross-correlation study, on the other hand, indicated a strong and positive association between Pc5 pulsations and solar wind velocity without lag for both geomagnetic activities.

Investigation of Pc5 pulsations effects and magnetospheric processes during intense geomagnetic storms

Sarup Khadka Saurav[1], Monika Karki[2], Binod Adhikari[1,3], Ashok Silwal[4], Luciano Aparecido Magrini[5], Ezequiel Echer[6], Odim Mendes[6], Margarete Oliveira Domingues[6], Sujan Prasad Gautam[4]

[1]Patan Multiple Campus, Tribhuvan University, Nepal
[2]Amrit Campus, Tribhuvan University, Nepal
[3]Department of Physics, St. Xavier's College, Tribhuvan University, Nepal
[4]Center for Space Plasma and Aeronomy Research, The University of Alabama in Huntsville, United States
[5]Federal Institute of São Paulo, São Paulo, Brazil
[6]National Institute for Space Research-INPE 12227-010 Sao Jose dos Campos, SP, Brazil

Key Points:

- The geomagnetic fluctuations recorded at low latitudes do not have locally generated attributes but they correspond to the global geomagnetic field variations possessing main sources in the magnetosphere and high latitude ionosphere.

- IMF B_z nominally influences the global Pc5 pulsations.

- The Pc5 Ipow has a relatively higher correlation with the solar wind velocity.

Corresponding author: Binod Adhikari, `binod.adhi@gmail.com`

Abstract

Giant pulsations belonging to the Pc5 frequency band were conceived by Rolf (1931). Such pulsations are influenced by magnetospheric processes produced by the solar wind. The purpose of this study is to investigate the Pc5 ULF waves and their relationship to solar parameters and geomagnetic indices, respectively, utilizing data from ground-based magnetometers and data provided by Operating Mission as Nodes on the Internet (OMNI). Magnetic observatories over Earth's surface reported intense long-period ULF activity on 19 February 2014 and 22-23 June 2015. We discovered a highly significant correlation between global Pc5 ULF waves and other interplanetary parameters, as well as a clear peak-to-peak correspondence during storms. We performed continuous wavelet transform (CWT) on the Pc5 integrated power (Ipow) and discovered that the majority of the intense Pc5 spectra are localized within the 64-256 minute Fourier period band. Our results suggest that geomagnetic fluctuations observed at low latitudes do not originate locally but rather are a reflection of global geomagnetic field variations with primary sources in the magnetosphere and high latitude ionosphere, which is consistent with the study of Gupta (1976). We discovered only nominal effects of IMF Bz on Pc5 pulsations, despite its southern counterpart being widely believed to be the principal driver of geomagnetic storms. Additionally, we discovered a moderate effect of solar wind pressure on Pc5 pulsations. Cross-correlation study, on the other hand, indicated a strong and positive association between Pc5 pulsations and solar wind velocity without lag for both geomagnetic activities. The Ipow on the ground increased in proportion to the speed of the solar wind. Our analysis supports the result of Kessel (2008) that the global toroidal modes of Pc5 fluctuations are caused by the K-H instability energizing the body type waveguide modes. This finding will aid in understanding some fundamental issues about the mechanism of Pc5 activity and the relationship between Pc5 waves and solar parameters.

Keywords: Geomagnetic Storms, Ultra Low Frequency Waves, Wavelet Analysis, Cross-correlation

1 Introduction

It is well established that there exists a one-to-one relationship between the interplanetary events and D_{st} events. A geomagnetic storm corresponds to an interval of time when a sufficiently high and enduring interplanetary convection electric field leads, through a substantial energization in the magnetosphere-ionosphere system, to an intensified ring current enough to surpass the threshold of quantifying storm time D_{st} index (W. Gonzalez et al., 1994). The southward interplanetary magnetic field (IMF B_s) has been defined as the primary cause of the geomagnetic storm. During geomagnetic storms, the solar-wind drivers of Pc5 pulsations are resolutely activated; therefore, such periods are important for the investigation of Pc5 wave generation mechanisms (Marin et al., 2014).

On sensitive magnetometers, the quasi-sinusoidal disturbance patterns are frequently observed, which have been attributed to hydromagnetic waves in the magnetosphere (Campbell, 1973; Kane, 1976). The characteristics of micropulsations are determined by the excitation of hydromagnetic (Alfven) waves at the magnetopause and in the magnetosphere, as well as their transmission to the Earth following absorption and partial reflection. Their activity in any region is dependent on the phase of the solar cycle, the seasons, the time of day, the ionospheric and magnetospheric conditions, and geomagnetic activity, in addition to the geographical latitude and longitude (Kane, 1976).

The establishment by Rolf (1931) of the concept of the giant pulsations belonging to the Pc5 group has been studied from different dimensions (for e.g. occurrences, characteristics, excitation mechanisms etc.), and more attention is being given now too. The solar wind is an important source of ground and magnetospheric Pc5 pulsations. Regarding the magnetospheric fluctuations, poloidal and toroidal Pc5 modes represent two limits of the hydromagnetic wave equations for standing waves on magnetic field lines (Kessel, 2008). The toroidal waves are driven by solar-wind at the magnetopause flanks. If the amplitudes are sufficiently large, then the waves are recorded on the ground. Ground station magnetometers sense the magnetospheric fluctuations that are modulated through the ionosphere. However, the signal may contain magnetotelluric effects on the ground that must be separated out to isolate those due to solar wind sources (Kessel, 2008).

Ultra low frequency (ULF) Pc5 pulsations characterize the longest hydromagnetic waves, which can oscillate in the Earth's magnetosphere. The interactions of solar wind with the geomagnetic field are influenced by such waves (Potapov et al., 2006). The mass, energy, and momentum movements in the magnetosphere are directly connected with the global ULF oscillations (Rae et al., 2005). Earlier studies have shown that Pc5 pulsations within low-frequency range 1.7 to 6.7 mHz, the intense and continuous activity of ULF wave observed at auroral latitudes, was followed within 1 to 2 days by superior fluxes of relativistic electrons (approximately Mev) at geosynchronous orbit (Rostoker et al., 1998; Baker et al., 1998; Mathie & Mann, 2001; I. Mann et al., 2004; Regi et al., 2015). The utmost solar wind driving environments are responsible for the global Pc5 waves that often occur throughout the whole duration of geomagnetic storms (Fei et al., 2006; Wang et al., 2020).

Various researchers have manifested that the ULF pulsations detected on the ground and within the magnetosphere are interrelated with the solar-wind conditions. For e.g., Mathie and Mann (2001) have discussed the correlation between solar wind speed and ULF pulsation power in the dayside magnetosphere for L shells in the range L=4-7, in support of the Kelvin-Helmholtz instability (KHI) as the driving mechanism. Other earlier studies, for e.g. Southwood (1968); Kivelson and Zu-Yin (1984); Claudepierre et al. (2008), have suggested KHI at magnetopause for describing Pc5 pulsations. The viscous shear interaction at the magnetopause as solar wind confronts the geomagnetic cavity results in the instability (Dunlop et al., 1994). I. R. Mann et al. (2002) have discussed the ground-based survey of field line resonances (FLR) characteristics by the use of high-frequency radar, geomagnetic and optical data. They found that KHI at the boundary layer generated discrete frequency global ULF wave activity during the interval of extreme solar-wind speed, perhaps by a discrete frequency magnetospheric waveguide mode, which is energized by the over reflection mechanism. Here the energy input for pulsations continues as long as the solar wind has a velocity greater than the critical velocity for instability (Samson et al., 1971). In summary, KHI generates the pulsations that are detected in the vicinity of dawn and dusk flank magnetopause (Claudepierre et al., 2008).

On the other hand, studies like Takahashi and Ukhorskiy (2008); Kepko and Spence (2003) have identified that the solar-wind pressure variations as the driving mechanism of ULF pulsations in the dayside magnetosphere. In that case, KHI plays only the secondary role as the source of pulsation energy. Takahashi and Ukhorskiy (2008) demonstrated that the solar-wind pressure variation had a relatively higher correlation with the Pc5 pulsations at geosynchronous orbit than the SW speed. They also suggested that the impact of pressure on the Pc5 waves is almost immediate. Moreover, the magnitude and orientation of the IMF often affect ULF variations in the Earth's convection electric field (Ridley et al., 1998; Claudepierre et al., 2008). These three mechanisms, discussed above, represent the external mechanism for driving ULF pulsations.

Many internal excitation mechanisms have been also proposed. These comprise drift wave instabilities operated by a pressure gradient between open and closed field lines within the Earth's magnetosphere (Hasegawa, 1971; Dunlop et al., 1994). The drift-bounce resonance, i.e. the drifting and bouncing motions of ring current ions by wave-particle interaction mechanisms, may also generate such waves (Southwood, 1976; Yamakawa et al., 2019). Here, we focus only on the external mechanisms, i.e. the effect of solar wind parameters on the Pc5 waves.

The investigation of micropulsation activity acquired from a global surface network assists to analyze the space weather, especially the variations of the solar-wind parameters in the interplanetary medium. We have taken two intense storms (peak D_{st} $\leq$-100 nT) cases to study Pc5 pulsations. The large amplitude oscillation of pulsations and high energy deposition into the magnetosphere and ionosphere are the unique features during the magnetic storm period. While studying the pulsations characteristics at different latitudes, the period-latitude and amplitude-latitude variations are noticeable. This paper investigates the variation of Pc5 pulsations from four ground magnetometer data and its relationship with plasma parameters and geomagnetic indices during two intense events.

The paper is organized as follows: in Section 2, the detailed information of selected sites and methods of the study are described. The result and discussion with possible clarification are provided in Section 4. Finally, in Section 5, the results of the study are concluded.

2 Datasets

A proper choice of events and magnetometer records (or geomagnetic related parameter, Ipow) can help us understand the Pc5 geomagnetic effects on the ground and the processes occurring in the magnetosphere boundary. We have selected two geomagnetic storms affected durations, i.e. 22-23 June 2015 and 19 February 2014. To find the geophysical condition of the selected durations, the D_{st} index (taken from `http://wdc.kugi.kyoto-u.ac.jp/dstdir/`) and the kp values (taken from `http://wdc.kugi.kyoto-u.ac.jp/kp/index.html`) have been used.
We have taken the major interplanetary parameters in this study. The significant parameter is initially the B_z because it propitiates two interaction regimes (south B_z implies frontal magnetic reconnection and north B_z implies laminar plasma flow regime, which could even evolve to turbulence characterized by KHI on the boundary). Similarly, B_y is related to reconnection via a magnetic configuration. The B_x component has also been taken into account. The IMF components data in the geocentric solar magnetospheric (GSM) coordinate system have been used. Complementary, at last, parameters like solar wind speed v_{sw} and solar wind flow pressure P_{sw} are fundamental parameters and are used. These data and geomagnetic indices have been taken from OmniWeb (`https://omniweb.gsfc.nasa.gov/`). The list of Richardson/Cane ICMEs has also been used.
On the ground data set, we have used the Pc5 integrated power (Ipow), the auroral geomagnetic index AE, and the low-latitude geomagnetic index Sym-H to evaluate the influence of every interplanetary parameter upon the surface effects in terms of the evolution of the electrodynamical coupling. The analyses implemented allow us to consider the influence even with the geomagnetic latitude, three high latitude stations (T42, RAN, and T41) and, for comparison, one low latitude station (TIR). The Pc5 Ipow data have been taken from superMAG (`http://supermag.jhuapl.edu/`) for four different stations listed in Table (1). The ionosphere modulates the ground-based fluctuations, so we focus on the integrated power discarding the waveform in comparison with plasma parameters. In the derivation of the ULF parameters, the N (local magnetic north) and E (local magnetic east) geomagnetic field components are used. The main field, or baseline, has been removed by the superMAG to subtract the daily variations and yearly trend.

Table 1. Geographic and geomagnetic location of the selected stations

Stations	IAGA	GLON (°)	GLAT (°)	MLON (°)	MLAT (°)
Tirunelveli	TIR	76.95	8.48	149.95	0.57
La Ronge	T42	254.74	55.2	-41.51	63.8
Rankine Inlet	RAN	267.89	62.82	-28.1	73.75
Kiana	T41	199.56	66.97	-105.56	65.59

3 Methodology

We examined the data using classical statistical cross-correlation analysis. However, we also selected specific wavelet transform techniques to deepen our investigation through wavelet using scale dependence correlation analysis. These analysis procedures allow us to investigate (and obtain comparisons of) the relationships below:

i. IMF-B_z, v_{sw}, P_{sw} versus Ipow
ii. AE, Sym-H versus Ipow

Based on the plots, we can analyze the role of different processes in the interplanetary medium on the Pc5 (Ipow) manifestations at higher latitude and additionally compare with the result at low latitude (station TIR).

3.1 Continuous Wavelet Transform (CWT)

Wavelet analysis, a method of time-scale localization, has been applied to 1-min data to study the periodicities of Pc5 time series. Here, we have used the non-orthogonal and complex Morlet wavelet function (mother wavelet), which is given as follows (Torrence & Compo, 1998):

$$\psi(x) = \pi^{-\frac{1}{4}} e^{i\omega_\circ x} e^{-\frac{x^2}{2}}, \tag{1}$$

where $\omega_\circ$ represents frequency. We have generated the family of continuously translated, dilated, and rotated wavelets from $\psi(x)$ (Farge, 1992):

$$\psi_{lx'\theta}(x) = l^{-\frac{n}{2}} \psi \left[\Omega^{-1}(\theta) \frac{x - x'}{l} \right], \tag{2}$$

where l and x' correspond to the width (scale parameter) and position of the wavelet, respectively. The rotation matrix Ω belongs to the group $SO(n)$ of rotation in R^n, and depends on the $n(n-1)/2$ Euler angles θ. The CWT of a distribution $f(x)$ gives wavelet coefficients (Farge, 1992):

$$\tilde{f}(l, x', \theta) = \int_{R^n} f(x) \psi^*{}_{lx'\theta}(x) d^n x, \tag{3}$$

where ψ^* represents complex conjugate of ψ. In Fourier space, the equation (3) becomes:

$$\tilde{f}(l, x', \theta) = \int_{R^n} \hat{f}(k) \psi^*{}_{lx'\theta}(k) d^n k \tag{4}$$

The time average of all the local wavelet spectra over certain period is the global wavelet spectrum (GWS). If the Fourier spectrum of the original time series is smoothed, then it approaches the GWS. The wavelet interpretation is referenced from Torrence and Compo (1998).

3.2 Cross-correlation analysis

Cross-correlation analysis, with coefficients ranging from -1 to 1, is the process of finding relation between two time series (Adhikari et al., 2018). It is the function of relative time between the signals i.e. the moment of time by which the signal has been shifted. The cross-correlation interpretation is referenced from Tsurutani et al. (1990) and Adhikari et al. (2018). The correlation between two series, P and Q, is given by Marques de Souza et al. (2018):

$$r = \frac{\sum(P_i - \bar{P}).\sum(Q_i - \bar{Q})}{\sqrt{\sum(P_i - \bar{P})^2 \sqrt{\sum(Q_i - \bar{Q})^2}}}, \tag{5}$$

where r denotes the correlation coefficient.

4 Results and Discussion

4.1 Solar activity and ULF wave during 22-23 June, 2015

The case study shown in Figure (1) exhibits the fluctuations in interplanetary parameters and ULF wave during 22-23 June in the year 2015. The magnetosphere got more disturbances from ∼6:00 UT on 22 June. Then, the large geomagnetic activities were observed as indicated by kp values, with a maximum value of 8+ among two days (not shown here in the plots). The higher kp value implies the greater energy input from the solar wind or solar particle radiation to the Earth. The ionospheric currents caused by enhanced activity in geomagnetic tail have principal contribution in the kp value (Piddington, 1968). Whereas D_{st} index indicated the disturbances rather later, i.e. from ∼16:00 UT on that day and the minimum value of D_{st} was -204 nT. The recovery phase extended over a week and shifted to quiet day value at ∼10:00 UT on 30 June. A cluster of shocks passed ACE satellite at 04:51 and 17:59 UT on 22 June, which were driven by the 19 June and the 21 June CMEs, respectively. An ICME (02:00 UT 23 June - 14:00 UT 24 June) was also preceded by 17:59 UT shock. In fact, there were three preceding shocks altogether, including the initial shock at 15:40 UT 21 June, and a single ICME. However, we have presented other two CMEs, that occurred during our selected interval, in Figure (1). The four CMEs altogether hit the Earth's magnetopause and the geomagnetic field activity ranged from quiet to severe storm conditions. Liu et al. (2015) recognized this multi-step development of geomagnetic storm as a *sheath-sheath-ejecta* scenario.

The Figure (1) exhibits the initial slow solar wind, the compressed average wind segment, followed by the compressed fast wind segment associated with a strong southward IMF component. As a result, we observed the growth of the IMF magnitude average ($|B|$). Such increase of IMF was the major parameter related to the beginning of geomagnetic substorms and storms (W. Gonzalez et al., 1994; W. D. Gonzalez et al., 1999). But we noticed drastic downward values of IMF-B_z during 18:39-19:44 UT. The threshold value (mentioned in W. Gonzalez et al. (1994)) of southward IMF ($-B_z$) for the intense storm, i.e. 10 nT, was crossed, but the threshold duration of 3 hours was not met for this event. The interplanetary magnetic-field lines are extended into Archimedes spirals by the merging of a radial component of solar-wind velocity and rotational motion of Sun (Parker, 1958). The solar-wind velocity is nearly radial in the vicinity of Earth, and it corresponds to the IMF motifs that rotates in conjunction with the Sun. However, the energy density associated with the streaming plasma is very much larger than the energy density of the interplanetary field in the interplanetary medium, so that the radial motion of the solar-wind plasma stretches out the interplanetary-field lines (Wilcox, 1968).
We observed the increase of flow pressure of solar wind (P_{sw}) from 05:45 UT on 22 June and sharp increase from 18:39 UT (in accordance with $P_{sw} = N.mv_{sw}^2$). The magnetosphere's outer boundary, the magnetopause, moves inward in response to increased solar wind dynamic pressure. This compression was also indicated by abrupt increase of Sym-H index in

the neighbourhood of that point (18:39 UT). This was the indication of a rise in dayside magnetopause currents prior to the onset of a storm. It corresponds to sudden storm commencement (SSC) since a magnetic storm followed the impulse. Then, the value of Sym-H continuously decreased and reached the lowest value of about -200 nT around 04:00 UT on 23 June. The negative Sym-H values were observed throughout 23 June. These conditions led to an intense storm. The Sym-H index ≤ -50 nT corresponds to the fluctuated geomagnetic field by its interaction with solar wind (W. Gonzalez et al., 1994; Adhikari et al., 2018). The southward oriented interplanetary magnetic field is responsible for the reduction in Sym-H value (Tsurutani et al., 1988). The AE-index increased earlier than other parameters, i.e. from 05:29 UT. Its sharp increase was from 14:06 UT, and the maximum value was noted to be 2698 nT at 20:09 UT on 22 June. The AE index characterizes the disturbances in the auroral electrojet current system. The AE index and IMF values became steady after 14:33 UT, 23 June.

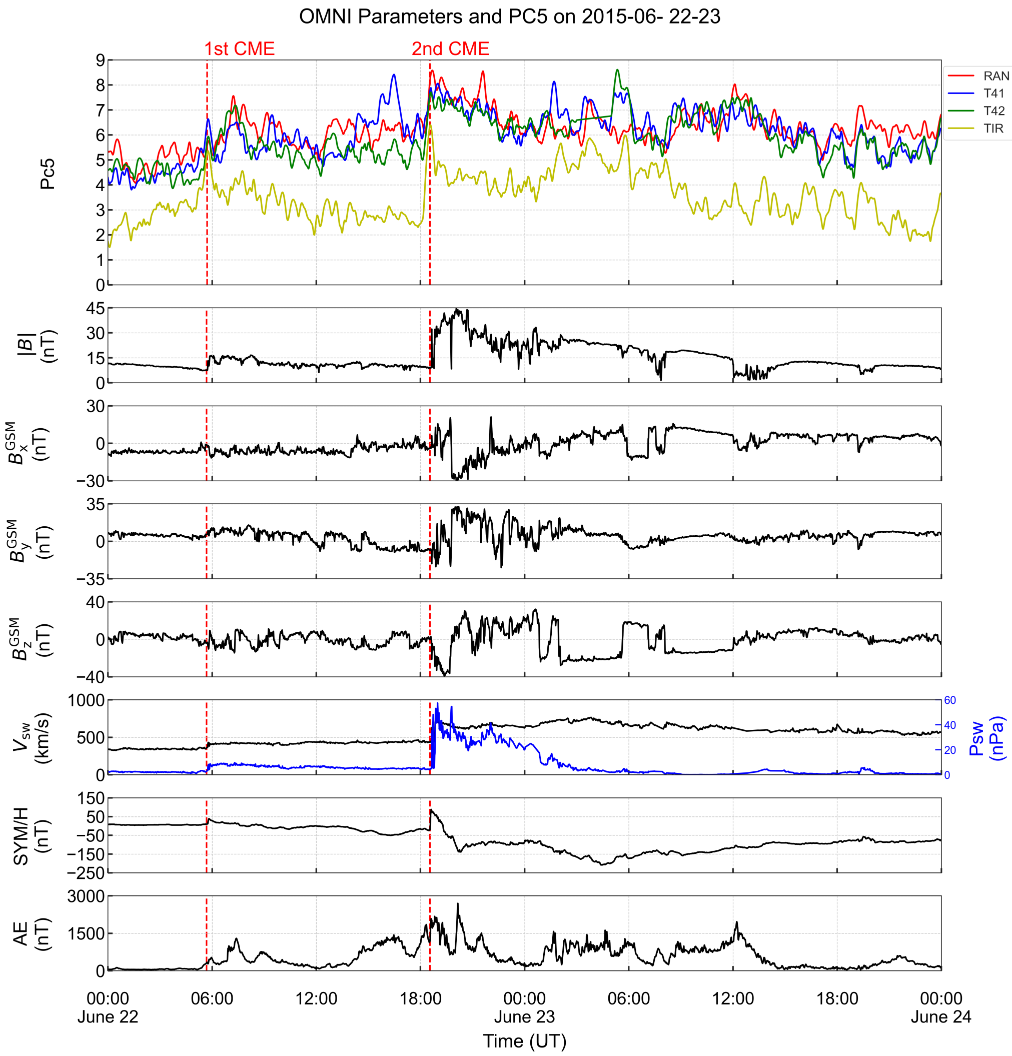

Figure 1. Variations of solar wind parameters, geomagnetic indices, and Pc5 pulsations: (a)Pc5 Ipow [Log (nT^2)] (b)IMF-$|B|$ (nT) (c)IMF-B_x (nT) (d)IMF-B_y (nT) (e)IMF-B_z (nT) (f)solar wind velocity $(km\ s^{-1})$ and solar wind flow pressure (nPa) (g)Sym-H index (nT) (h)AE index (nT) during 22-23 June, 2015

.

The first panel of Figure 1 shows the Pc5 wave activity at four different observatories. The ULF power index, calculated using the data of worldwide distributed magnetometers, indicates the global wave power intensity in the Pc5 frequency band (Kozyreva et al., 2007; Pilipenko et al., 2010). The global spatial compositions of Pc5 pulsations were disparate for June 22 and 23: on 22 June, the maximal intensity was observed in all magnetometer stations at ∼07:30 UT in early morning hours, whereas in post noon hours, very intense Pc5 waves were observed at ∼18:30 UT. On 23 June, Pc5 activity started after the storm main phase and spread to the morning, noon, and afternoon hours. Comparing global ULF activity with other interplanetary parameters showed (in a general shape) a well-pronounced peak-to-peak correspondence during the storm. The high magnitude fluctuations (maximum Ipow = 9 Log (nT^2)) of Pc5 pulsations were observed in T41, RAN, and T42 stations, whereas relatively low magnitude in the TIR station. The nature of the pulsations is similar in all stations. The principal characteristics of geomagnetic variation phenomena observed at low latitudes were not locally generated, but rather manifestations of global field variations having their main sources in the magnetosphere and high latitude ionosphere (Gupta, 1976).

It is generally accepted that the interaction between the streaming solar-wind plasma and the magnetosphere produces hydromagnetic waves in the Pc5 period range. The tangential stresses are produced at the flanks of the boundary layer near the dawn and dusk meridians when tumultuous solar wind moves away from the subsolar point within the magnetosheath. These stresses can give rise to waves produced by the KHI. The generated waves are directed towards the Earth along the magnetic field lines, which intersect the ionosphere in the auroral oval region (Gupta, 1976).

4.2 Solar activity and ULF wave on 19 Feb, 2014

Figure (2) represents the fluctuations in interplanetary parameters and ULF wave during the intense storm on 19 February 2014. The onset of storm was from ∼21:00 UT on Feb 18 (D_{st} index -27 nT during this hour) and minimum D_{st} value was -119 nT, observed on Feb 19. Its recovery phase extended upto 05:00 UT of 23 February. The currents within the magnetosphere and ionosphere are escalated during the enhanced level of solar wind-magnetosphere interaction. These current systems characterize the magnetic bays. The storm time disturbances of the geomagnetic field, D_{st} index, describes the variation of equatorial ring current (Mendes Jr et al., 2005). The amplitude of the D_{st} event is asserted to be associated with the large amplitude, long duration, negative B_z event following the shock (W. D. Gonzalez & Tsurutani, 1987). The magnetospheric disturbances were from the starting time of our selected day. The finalized kp value got lowered from 15-18 UT (kp index 2+) on 19 February, although there were disturbances on 20 February. The maximum kp index was 6+. This intense geomagnetic storm was the result of two powerful interplanetary CMEs (15:00 UT 18 Feb - 07:00 UT 19 Feb; 12:00 UT 19 Feb - 03:00 UT 20 Feb).

The v_{sw} and P_{sw} showed the simultaneous growth from 03:57 UT on Feb 19. The solar wind velocity of 506.4 $km\ s^{-1}$ was noted at 12:04 UT. The peak period for solar wind flow pressure was observed to be 12:04 UT (5.19 nPa) -14:38 UT (4.77 nPa). The IMF B_z immediately reduced after the interplanetary shock at 03:09 UT 19 Feb. During the southward B_z interval, the high-level AE activity was observed that was related to convection enhancement caused by the growth of solar wind velocity via magnetic reconnection, and/or by the large-amplitude values of IMF B_y component, via a B_y dominant reconnection process (W. D. Gonzalez & Tsurutani, 1987). The entire northward values were observed from 13:38 - 22:54 UT on that day. The negligible AE activity was associated with the positive B_z duration. This third component, B_z, of the interplanetary magnetic field is perpendicular to the ecliptic and is created by waves and other disturbances in the solar wind (W. Gonzalez et al., 1994). The Sym-H showed a slight decrease and then quick growth from 03:57 UT. The Sym-H minimum value was observed to be -120 nT around 07:00 UT. This value then

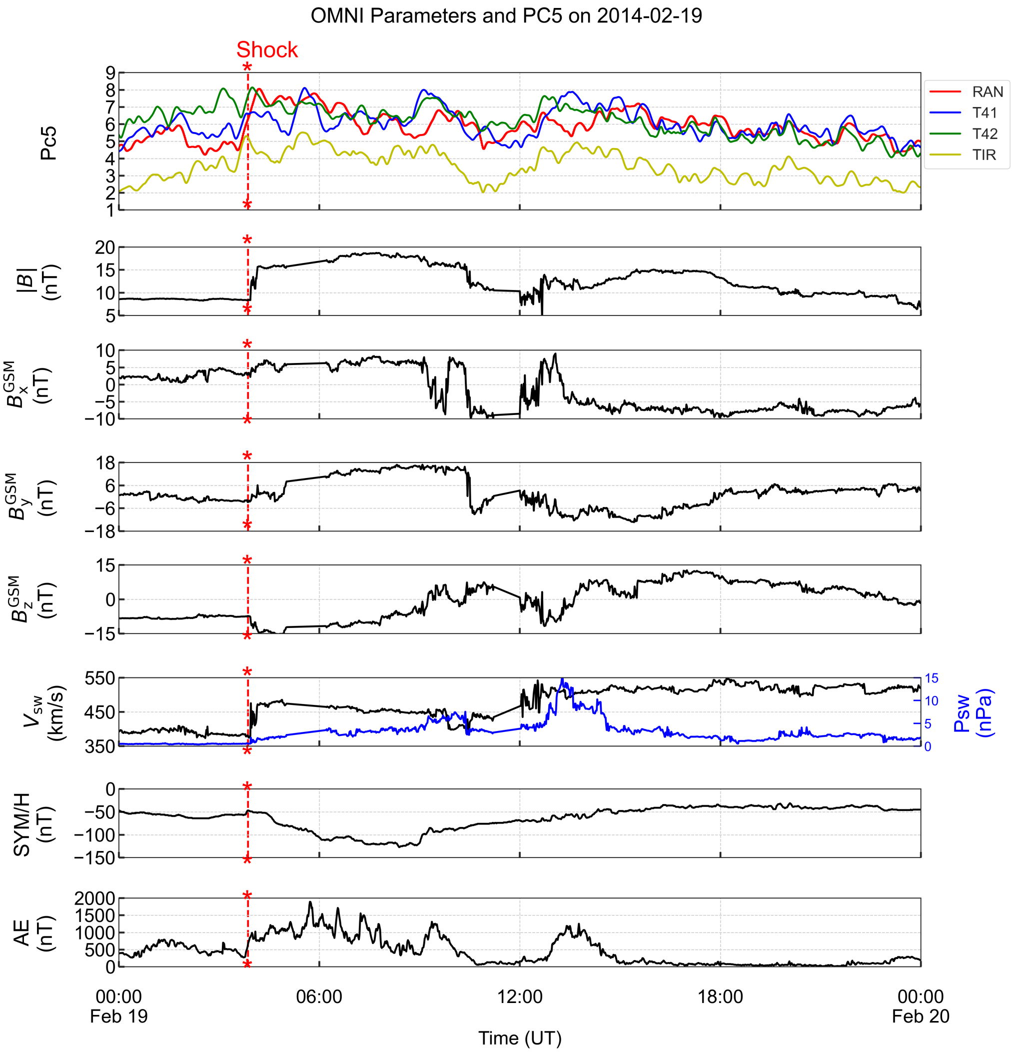

Figure 2. Variations of solar wind parameters, geomagnetic indices, and Pc5 pulsations (a)Pc5 Ipow [Log (nT^2)] (b)IMF $|B|$ (nT) (c)IMF B_x (nT) (d)IMF B_y (nT) (e)IMF B_z (nT) (f)solar-wind velocity ($km\ s^{-1}$) and flow pressure (nPa) (g)Sym-H index (nT) (h)AE index (nT) on 19 Feb 2014
.

recovered to the normal level after 13:00 UT. During the main phase of geomagnetic storms, charged particles are energized near the Earth plasma sheet and injected deeper into the magnetosphere (Adhikari et al., 2018).

The first panel of Figure (2) exhibits the enhancement of amplitude with discontinuities that occur in the signal and observe abrupt changes in the signal. Here, we again observed low Ipow values at low latitude station TIR. However, TIR records highlighted the clear effects of B_z Northward versus solar wind speed (for instance about 10:00 - 11:00 UT). The global Pc5 Ipow was decayed from high to low geographic latitudes. The integrated power exceeded the value of 9 Log (nT^2) during the main storm phase in T41, RAN, and T42 stations. The large amplitude fluctuations and few sinusoidal nature were observed, making it more suitable for wavelet analysis. These large amplitude global Pc5 pulsations are the major component of the tail dynamics during periods of enhanced convection (Lyons et al.,

2002; Ngwira et al., 2018).
The Pc5 integrated power is enhanced during the main phase of geomagnetic storms. The pulsation power can be used as an indicator of the initial passage of a high-speed solar wind stream past Earth (Engebretson et al., 1998). It is apparent that the solar wind speeds of less than ∼400 $km\ s^{-1}$ do not give rise to appreciable pulsation power, while the 400-500 $km\ s^{-1}$ regimes seem to give rise to pulsation power. These moderate solar-wind speed conditions influence the pulsation power because some of the pulsations may be driven by an energy source with a weaker dependence on solar wind speed, such as intervals of reconnection during southward IMF B_z or very large solar wind impulses delivered by the dynamic pressure changes (Mathie & Mann, 2001). Above 500 $km\ s^{-1}$, we observed significant growth of Pc5 pulsation power.

4.3 CWT analysis

4.3.1 Spectral analysis of Pc5 Ipow during 22 and 23 June 2015

The wavelet power spectrum of the T41 station shows that most of the power was localized in the Fourier period band of 64-256 minutes. There were high Pc5 activities during 400-2100 minutes, although some activities were on both sides of this duration. During 400-2100 minutes, the Pc5 intensification was observed. It was also affected by the edge effect at its initial phase. Such continuous intensification during the storm is responsible for the deposition of a higher energy into the magnetospheric and ionospheric systems through Joule heating (Dunlop et al., 1994). The most fluctuated parameter was AE-index than other included parameters during this period. We took a red noise process (power directly proportional to time periods) as the background spectrum to determine the significance level, the thick contours in the power spectrum. Figure (3) represents the regions of more than 95% confidence level. There were no significant regions in the wavelet power spectrum in the few initial hours and during 2100-2400 minutes.

Taking a red noise process, each point in the wavelet power spectrum is χ_2^2 distribution assuming the original Fourier components are normally distributed. The green dashed line on scale average time series is the 95% confidence level red noise spectrum for $\alpha = 0.72$. The lowest variance was observed from starting time upto 200 minutes. Two broad maxima were observed during 950-1100 min and 1500-2000 min. It can be clearly seen that there was a random distribution of variance from the mean, and also, the clusters in the power spectrum are distributed around the whole duration. It implies the randomness of our data. In the GWS, the dashed line is the 95% confidence level line, and it is seen that only a few lines are out of it. The GWS also supported the 64-256 minutes Fourier period of time series during the storm. It should be noted that the global wavelet spectrum provides a consistent and unbiased estimation of the true power spectrum of the time series (Torrence and Compo (1998) and reference therein). The peaks found on the GWS plot show the main periodicities of the Pc5 Ipow. The maximum power was observed to be ∼18 Log (nT^2) associated with the optimum periodicity (256 min) on the GWS plot.
The wavelet power spectrum of RAN showed less Pc5 activities during 1400-1600 min and intense activities on both sides this duration with Fourier period of 64-192 min band. The GWS also supported this, and the maximum power was observed to be ∼10 Log (nT^2). The high variances were recorded during 1000-1400 min of the event duration. The wavelet power spectrum of the T42 station indicated a single, rather than the long, continuous, and some energetic short-term intensifications. We can see that the localization is gradually shifted to the lower Fourier period band. The peak in the variances was observed during 1600-1900 min. The low latitude station TIR had only energetic short term intensification as shown in Figure (3) and the peak intensification during 1000-1200 min. The GWS showed the least main periodicity among the four stations.

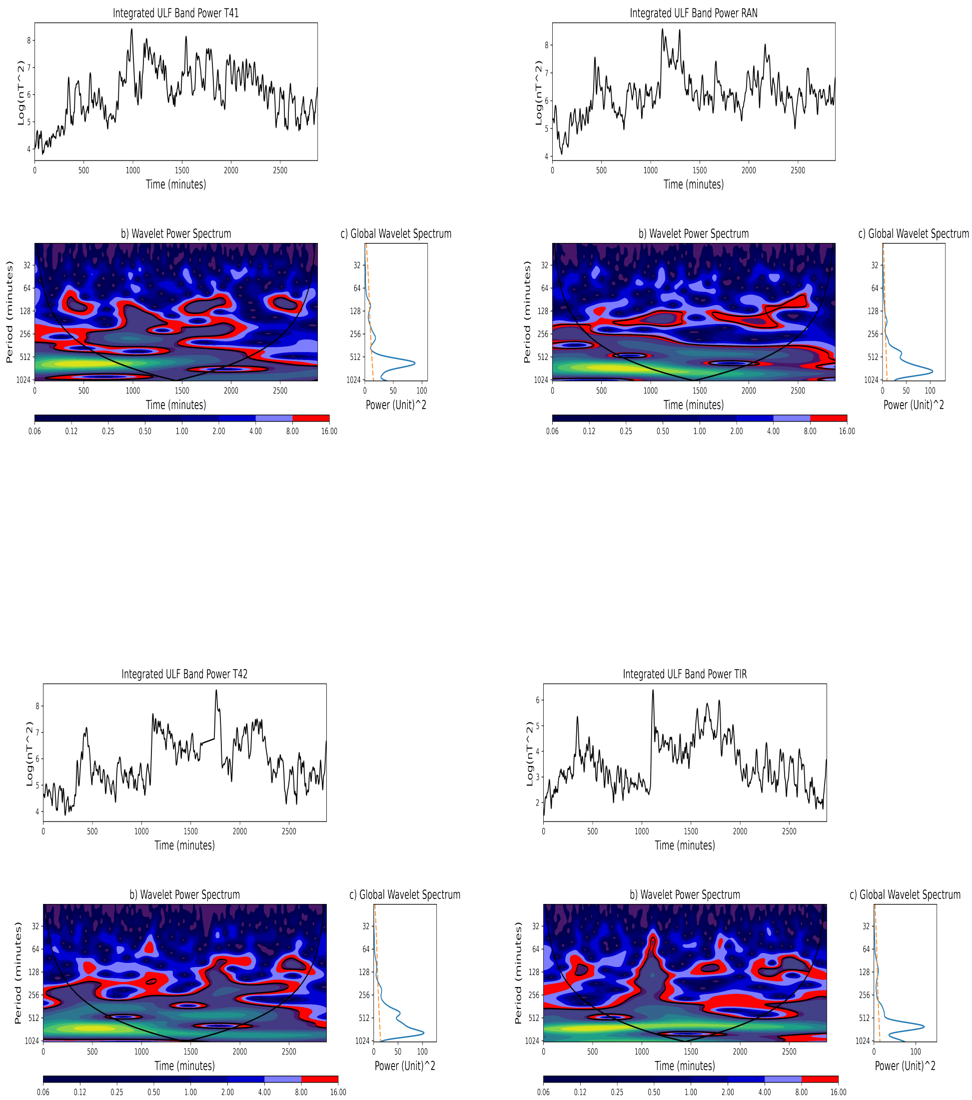

Figure 3. Integrated power, scalogram, and global wavelet spectrum (GWS) of Pc5 pulsations observed at (a)T41 (top left) (b)RAN (top right) (c)T42 (bottom left) (d)TIR (bottom right) stations during 22 and 23 June, 2015

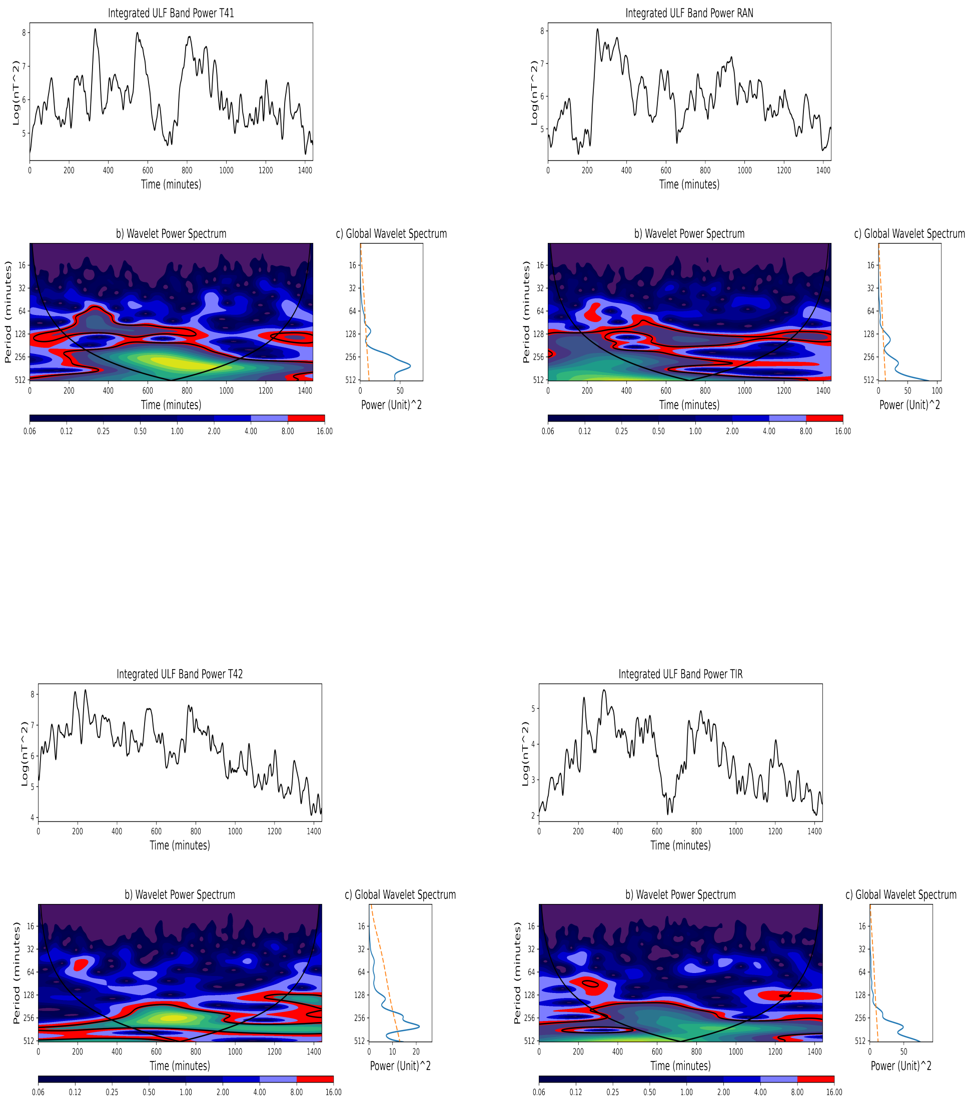

Figure 4. Integrated power, scalogram, and global wavelet spectrum (GWS) of Pc5 pulsations observed at (a)T41 (top left) (b)RAN (top right) (c)T42 (bottom left) (d)TIR (bottom right) stations on 19 Feb, 2014

4.3.2 Spectral analysis of Pc5 on 19 Feb, 2014

The wavelet power spectrum of Pc5 time-series at T41 station (highest geographic latitude station among selected), Figure (4), indicated the higher amplification of Ipow during 200-1000 min on Feb 19. This was continuous intensification, localized within the Fourier period band of 64-256 min. We can clearly see the higher variances during this period. Also another signature of intensification was noted after 1200 min, whose most parts were not included inside the cone of influence. The GWS indicated the maximum power of ∼40 Log (nT^2), associated with the highest periodicity.
We observed the intense activities at RAN also during the 1000-1200 min, the low activity duration of T41. A single energetic short-term intensification was also observed. The GWS showed the relatively lower power and rather decrease of main periodicity than those at T41. While at T42, we can clearly see the gradual decrease of Fourier period band of intensed localization in comparison to that at T41 and RAN. And the low variance fluctuations were frequent at T42 during this event. The wavelet power spectrum of low latitude station TIR (Figure (4)) showed the tendency of short-term intensification. These were obtained during 200-400 min and 1100-1200 min on Feb 19. There were also lower variances as in T42. The GWS indicated the maximum power of ∼20 Log (nT^2).

4.4 Cross-correlation analysis

We observed peak to peak correspondence between solar wind parameters and Pc5 Ipow from time series analysis. To explore further relations between them, as a function of displacement of one series relative to the other by units of time, we have taken results from cross-correlation analysis. For the 22 June event, the variation of cross-correlation coefficients with time is shown in Figure (5), where Pc5 Ipow, solar wind parameters, and geomagnetic indices are used. The positive correlation, with maximum cross-correlation coefficient 1 at lag 0 min, was seen in Pc5-v_{sw} case. This implied the same Pc5 Ipow and solar wind velocity phase in all selected stations with the maximum coefficient. In auto-correlation, there is always a peak at a lag of zero if the signal is not a trivial zero signal (Usoro et al., 2015). This also supports a strong correlation of observed solar wind velocity and the Pc5 Ipow time series. The maximum coefficient ∼0.65 was obtained for T41, RAN, and T42 stations without lag, whereas the maximum value was ∼0.7 for TIR with a response time, in Pc5-solar wind flow pressure correlation. It is worth noting that the perturbations in P_{sw} are responded by the Pc5 Ipow with a time delay in the low latitudinal station. Consequently, we interpreted that the geomagnetic fluctuations recorded at low latitudes did not have locally generated attributes but they corresponded to the global geomagnetic field variations possessing main sources in the magnetosphere and high latitude ionosphere. We observed the relatively low correlation of IMF B_z, maximum coefficient of ∼0.3 with a shift in time, with Pc5 time series. The positive correlation, with maximum cross-correlation coefficient ∼0.8 at lag 0 min, was seen for the Pc5-AE case. But the Pc5 was negatively correlated with Sym-H, with the maximum coefficient of -0.8 at lag 0 min.

We observed similar cross-correlation results also for 19 Feb 2014 (Figure (6)). The Pc5 Ipow was positively correlated with both the solar wind velocity and the flow pressure, same as in the June event with maximum coefficients of 1 and 0.8 at lag 0 min, respectively. This implies that the Pc5 Ipow was directly proportional to the solar wind velocity and the flow pressure. Moreover, they were in the same phase at 0 min lag, but a relatively stronger correlation of Pc5 Ipow with solar wind velocity than the flow pressure was observed. The maximum cross-correlation coefficient of ∼0.5 was seen in the Pc5-IMF B_z correlation. The IMF B_z showed less correlation with Pc5 integrated power, although it was the primary cause for the onset of geomagnetic storms. The Pc5 Ipow was positively correlated with the AE index with maximum coefficients of 0.8 at lag 0 min. While Pc5 was negatively correlated with Sym-H with a maximum coefficient of -0.9 at lag 0 min. This implies their

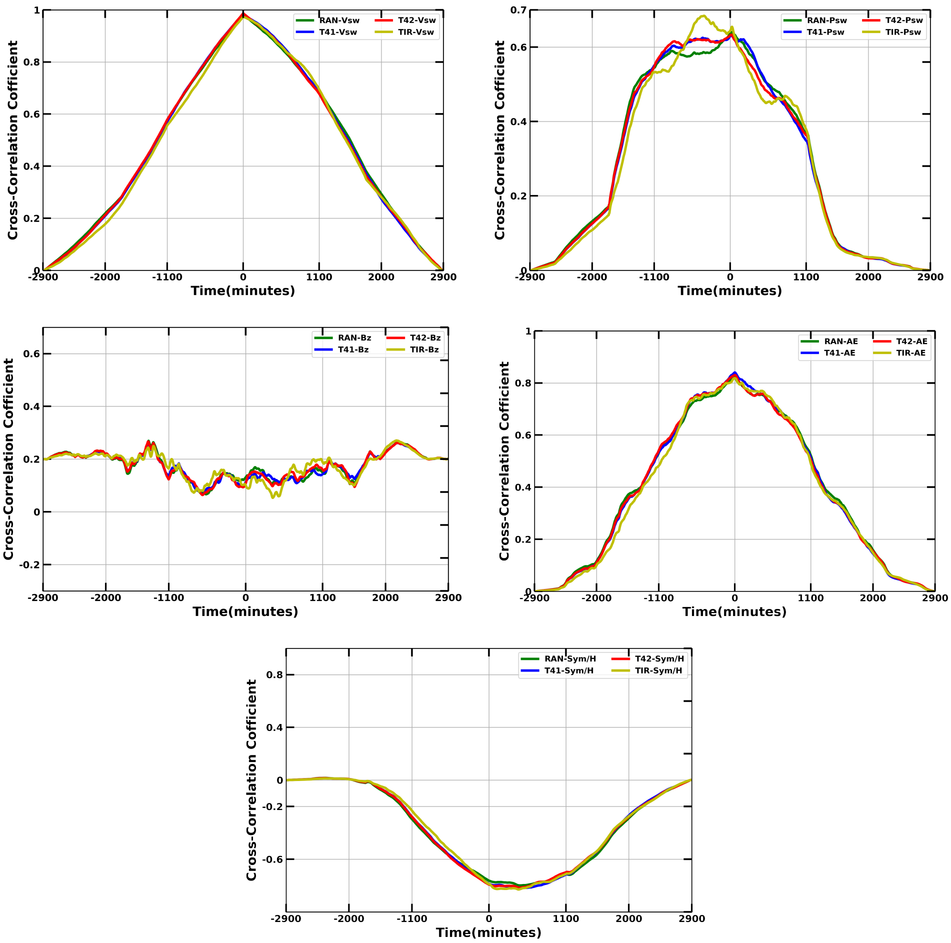

Figure 5. Cross-correlation of Pc5 Ipow with solar wind parameters for four stations T41, RAN, T42, and TIR (a)Pc5-solar wind velocity (b)Pc5-solar wind flow pressure (c)Pc5-IMF B_z (d)Pc5-AE index (e)Pc5-Sym-H index during 22 and 23 June, 2015

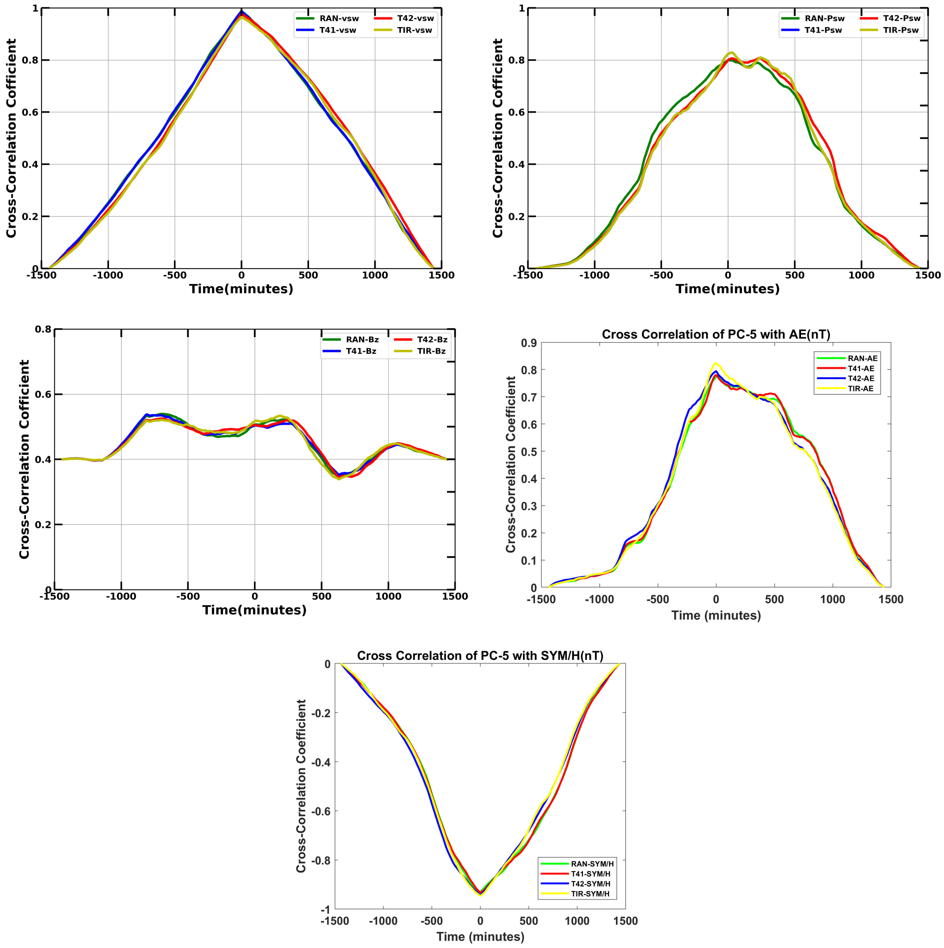

Figure 6. Cross-correlation of Pc5 Ipow with solar wind parameters for four stations T41, RAN, T42, and TIR (a)Pc5-solar wind velocity (b)Pc5-solar wind flow pressure (c)Pc5-IMF B_z (d)Pc5-AE index (e)Pc5-Sym-H index on 19 Feb, 2014

inverse proportionality.

It is apparent that the solar wind speed controls the Pc5 pulsation activity. We observed the immediate response of Pc5 pulsations to the perturbations that occur in the v_{sw} as indicated by the lag 0 min. The positive time lag in Figures (5) and (6) has no physical meaning because it would mean that the geomagnetic consequences happened before the perturbations on solar wind parameters. The energy contained in the solar wind enters the magnetosphere and appears as hydromagnetic energy. The interplanetary source mechanisms are frequency-dependent for hydromagnetic energy production in the magnetosphere.

Besides the v_{sw}, the angle θ_{xB} between the IMF vector and the Earth-Sun line plays a crucial role in the variations in observed geomagnetic activity, known as the angle effect. The waves generated beyond the Earth's bow shock are transferred to the magnetopause and subsequently toward the ground for small θ_{xB}. This mechanism has a contribution only to the high-frequency band. The effects of velocity become dominant for the low-frequency surface field fluctuations (Wolfe et al., 1980). The angle effect is IMF dependent mechanism. The cross-correlation analysis found that the IMF B_z magnitude and orientations have only a little influence on the Pc5 Ipow. This implies the possibility of their occurrence even in the IMF B_z orientation when the transmission of solar-wind energy flux to the magnetosphere, by a process of reconnection of IMF and the magnetospheric magnetic field, is quelled (Marin et al., 2014). The global excitation of Pc5 pulsations may be a significant medium of the energy transmission from the solar wind into the magnetosphere during such orientation (Potapov et al., 2009).

We observed the moderate effect of solar-wind pressure on the Pc5 pulsations. The fast-mode magnetosonic waves and shear-Alfven waves are imparted into the inner magnetosphere when the fluctuations in solar-wind pressure concern the magnetopause. Such waves are guided along the direction of the Poynting flux. The pressure fluctuations excite a response within the magnetosphere and on the ground, across a broad range of solar wind speed and pressure, and IMF B_z. The solar wind pressure variations dominantly drive the Pc5 compressional fluctuations (Kessel, 2008). It may be further interpreted based on the cavity model. The magnetosphere behaves as a resonant cavity within this model. The compressional waves with the frequencies equivalent to that of the cavity are excited by the sudden changes in the solar wind's pressure. This compressional wave then excites a field line resonance (FLR) (Eriksson et al., 2006). It is worth noting that the ULF pulsations generated by the various mechanisms are thought to occur primarily over different but sometimes overlapping.
In consistent with the studies like (Mathie & Mann, 2001; Engebretson et al., 1998), our results support the velocity-dependent mechanism as the source of pulsation energy than the dynamic pressure and IMF dependent mechanisms. The close correlation between intervals of enhanced solar wind speed and growth in pulsation power strongly support the magnetopause KHI as the probable source of pulsation energy (Mathie & Mann, 2001). The solar wind velocity greater than the critical velocity of instability can drive large amplitude oscillations by the KHI mechanism. These pulsations are the result of fully developed surface waves propagating on the magnetospheric boundary (Junginger & Baumjohann, 1988).

Our results advocate that the ground Pc5 fluctuations are attributed to the KHI for the selected intervals. The KHI occurs at the interface between two fluids in relative motion. The fast magnetosheath flow excites surface waves on the boundary layer that are suitable to KHI. The global modes of Pc5 fluctuations, having the driving and response frequencies mainly in the range 0.5 to 4 mHz, are compatible with cavity and waveguide eigenfrequencies. The integrated power on the ground and in the magnetosphere growths with the solar-wind speed, and toroidal fluctuations dominate the magnetopause flanks. As a consequence, we detected the geomagnetic fluctuations in the Pc5 frequency band. These observations support a K-H instability energizing the body type waveguide modes (Kessel, 2008).

5 Conclusions

After studying Pc5 characteristics during two intense geomagnetic storms, especially focusing on spectral analysis and cross-correlation with solar wind parameters, our key findings are:

i. The geomagnetic fluctuations recorded at low latitudes do not have locally generated attributes but they correspond to the global geomagnetic field variations possessing main sources in the magnetosphere and high latitude ionosphere. Moreover, the global Pc5 Ipow is decayed from high to low geographic latitudes.
ii. IMF B_z nominally influences the global Pc5 pulsations. This implies the possibility of their occurrence even in the IMF B_z orientation when the transmission of solar-wind energy flux to the magnetosphere, by a process of reconnection of IMF and the magnetospheric magnetic field, is quelled. The global excitation of Pc5 pulsations may be a significant medium of the energy transmission from the solar wind into the magnetosphere during such orientation (Potapov et al., 2009).
iii. The Pc5 Ipow has a relatively higher correlation with the solar wind velocity than with flow pressure for here included two cases. The Pc5 Ipow and the solar wind velocity almost behaved as a single parameter at lag 0 min, assuming both are normally distributed. The global modes of Pc5 fluctuations, having the driving and response frequencies mainly in the range 0.5 to 4 mHz, are compatible with cavity and waveguide eigenfrequencies. The integrated power on the ground increases with the solar wind speed, and toroidal fluctuations dominate the magnetopause flanks. These observations support a K-H instability energizing the body type waveguide modes (Kessel, 2008).
iv. Most intense Pc5 spectra are localized within the Fourier period band of 64-256 minutes. The Fourier period band of the intense Pc5 Ipow spectrum tends to decrease if the geographic latitude is lowered and vice-versa. Both long and short intensification of Pc5 Ipow is present in high latitude stations, whereas only the solitary waves are frequent in low latitudes for the same event.

Acknowledgments

We thank our data sources superMAG (`http://supermag.jhuapl.edu/`) and OMNIweb (`https://omniweb.gsfc.nasa.gov/`). We are grateful to the referees for their constructive comments.

We gratefully acknowledge National Science and Research Socity (NSRS) for their support. We thank Nirmal Dangi, Ganga Prasad Adhikari, Hari Ram Krishna Gauli, Krishna Prasad Paudel, and Tek Bahadur Khadka for some fruitful discussions about this project.

References

Adhikari, B., Dahal, S., Sapkota, N., Baruwal, P., Bhattarai, B., Khanal, K., & Chapagain, N. P. (2018). Field-aligned current and polar cap potential and geomagnetic disturbances: A review of cross-correlation analysis. *Earth and Space Science*, *5*(9), 440-455. doi: 10.1029/2018EA000392

Baker, D., Pulkkinen, T., Li, X., Kanekal, S., Blake, J., Selesnick, R., . . . Rostoker, G.

(1998). Coronal mass ejections, magnetic clouds, and relativistic magnetospheric electron events: Istp. *Journal of Geophysical Research: Space Physics*, *103*(A8), 17279–17291. doi: https://doi.org/10.1029/97JA03329

Campbell, W. (1973). Research on geomagnetic pulsations from january 1969 to july 1972—a review. *Journal of Atmospheric and Terrestrial Physics*, *35*(6), 1147–1157. doi: https://doi.org/10.1016/0021-9169(73)90011-1

Claudepierre, S. G., Elkington, S. R., & Wiltberger, M. (2008). Solar wind driving of magnetospheric ulf waves: Pulsations driven by velocity shear at the magnetopause. *Journal of Geophysical Research: Space Physics*, *113*(A5). doi: https://doi.org/10.1029/2007JA012890

Dunlop, I., Menk, F., Hansen, H., Fraser, B., & Morris, R. (1994). A multistation study of long period geomagnetic pulsations at cusp and boundary layer latitudes. *Journal of atmospheric and terrestrial physics*, *56*(5), 667–679. doi: https://doi.org/10.1016/0021-9169(94)90106-6

Engebretson, M., Glassmeier, K.-H., Stellmacher, M., Hughes, W. J., & Lühr, H. (1998). The dependence of high-latitude pcs wave power on solar wind velocity and on the phase of high-speed solar wind streams. *Journal of Geophysical Research: Space Physics*, *103*(A11), 26271-26283. doi: https://doi.org/10.1029/97JA03143

Eriksson, P., Walker, A., & Stephenson, J. (2006). A statistical correlation of pc5 pulsations and solar wind pressure oscillations. *Advances in Space Research*, *38*(8), 1763–1771. doi: https://doi.org/10.1016/j.asr.2005.08.023

Farge, M. (1992). Wavelet transforms and their applications to turbulence. *Annual review of fluid mechanics*, *24*(1), 395–458. doi: https://doi.org/10.1146/annurev.fl.24.010192.002143

Fei, Y., Chan, A. A., Elkington, S. R., & Wiltberger, M. J. (2006). Radial diffusion and mhd particle simulations of relativistic electron transport by ulf waves in the september 1998 storm. *Journal of Geophysical Research: Space Physics*, *111*(A12). doi: https://doi.org/10.1029/2005JA011211

Gonzalez, W., Joselyn, J.-A., Kamide, Y., Kroehl, H. W., Rostoker, G., Tsurutani, B., & Vasyliunas, V. (1994). What is a geomagnetic storm? *Journal of Geophysical Research: Space Physics*, *99*(A4), 5771–5792. doi: https://doi.org/10.1029/93JA02867

Gonzalez, W. D., & Tsurutani, B. T. (1987). Criteria of interplanetary parameters causing intense magnetic storms (dst <-100 nt). *Planetary and Space Science*, *35*(9), 1101-1109. doi: https://doi.org/10.1016/0032-0633(87)90015-8

Gonzalez, W. D., Tsurutani, B. T., & De Gonzalez, A. L. C. (1999). Interplanetary origin of geomagnetic storms. *Space Science Reviews*, *88*(3-4), 529–562. doi: https://doi.org/10.1023/A:1005160129098

Gupta, J. C. (1976). Some characteristics of large amplitude pc5 pulsations. *Australian Journal of Physics*, *29*(2), 67–88. doi: https://doi.org/10.1071/PH760067

Hasegawa, A. (1971). Plasma instabilities in the magnetosphere. *Reviews of Geophysics*, *9*(3), 703-772. doi: https://doi.org/10.1029/RG009i003p00703

Junginger, H., & Baumjohann, W. (1988). Dayside long-period magnetospheric pulsations: Solar wind dependence. *Journal of Geophysical Research: Space Physics*, *93*(A2), 877-883. doi: https://doi.org/10.1029/JA093iA02p00877

Kane, R. (1976). Geomagnetic field variations. *Space Science Reviews*, *18*(4), 413–540. doi: https://doi.org/10.1007/BF00217344

Kepko, L., & Spence, H. E. (2003). Observations of discrete, global magnetospheric oscillations directly driven by solar wind density variations. *Journal of Geophysical Research: Space Physics*, *108*(A6). doi: https://doi.org/10.1029/2002JA009676

Kessel, R. L. (2008). Solar wind excitation of pc5 fluctuations in the magnetosphere and on the ground. *Journal of Geophysical Research: Space Physics*, *113*(A4). doi: https://doi.org/10.1029/2007JA012255

Kivelson, M. G., & Zu-Yin, P. (1984). The kelvin-helmholtz instability on the magnetopause. *Planetary and space science*, *32*(11), 1335–1341. doi: https://doi.org/10.1016/0032-0633(84)90077-1

Kozyreva, O., Pilipenko, V., Engebretson, M., Yumoto, K., Watermann, J., & Romanova, N. (2007). In search of a new ulf wave index: Comparison of pc5 power with dynamics of geostationary relativistic electrons. *Planetary and Space Science*, *55*(6), 755–769. doi: https://doi.org/10.1016/j.pss.2006.03.013

Liu, Y. D., Hu, H., Wang, R., Yang, Z., Zhu, B., Liu, Y. A., ... Richardson, J. D. (2015, aug). PLASMA AND MAGNETIC FIELD CHARACTERISTICS OF SOLAR CORONAL MASS EJECTIONS IN RELATION TO GEOMAGNETIC STORM INTENSITY AND VARIABILITY. *The Astrophysical Journal*, *809*(2), L34. doi: 10.1088/2041-8205/809/2/l34

Lyons, L., Zesta, E., Xu, Y., Sánchez, E., Samson, J., Reeves, G., ... Sigwarth, J. (2002). Auroral poleward boundary intensifications and tail bursty flows: A manifestation of a large-scale ulf oscillation? *Journal of Geophysical Research: Space Physics*, *107*(A11), SMP–9. doi: https://doi.org/10.1029/2001JA000242

Mann, I., O'Brien, T., & Milling, D. (2004). Correlations between ulf wave power, solar wind speed, and relativistic electron flux in the magnetosphere: Solar cycle dependence. *Journal of Atmospheric and Solar-Terrestrial Physics*, *66*(2), 187–198. doi: https://doi.org/10.1016/j.jastp.2003.10.002

Mann, I. R., Voronkov, I., Dunlop, M., Donovan, E., Yeoman, T. K., Milling, D. K., ... Opgenoorth, H. J. (2002). Coordinated ground-based and cluster observations of large amplitude global magnetospheric oscillations during a fast solar wind speed interval. *Annales Geophysicae*, *20*(4), 405–426. doi: 10.5194/angeo-20-405-2002

Marin, J., Pilipenko, V., Kozyreva, O., Stepanova, M., Engebretson, M., Vega, P., & Zesta, E. (2014). Global pc5 pulsations during strong magnetic storms: excitation mechanisms and equatorward expansion. In *Annales geophysicae* (Vol. 32, pp. 319–331). doi: https://doi.org/10.5194/angeo-32-319-2014

Marques de Souza, A., Echer, E., Bolzan, M. J. A., & Hajra, R. (2018). Cross-correlation and cross-wavelet analyses of the solar wind imf b_z and auroral electrojet index ae coupling during hildcaas. *Annales Geophysicae*, *36*(1), 205–211. doi: https://angeo.copernicus.org/articles/36/205/2018/

Mathie, R. A., & Mann, I. R. (2001). On the solar wind control of pc5 ulf pulsation power at mid-latitudes: Implications for mev electron acceleration in the outer radiation belt. *Journal of Geophysical Research: Space Physics*, *106*(A12), 29783-29796. doi: https://doi.org/10.1029/2001JA000002

Mendes Jr, O., Domingues, M. O., Da Costa, A. M., & De Gonzalez, A. L. C. (2005). Wavelet analysis applied to magnetograms: Singularity detections related to geomagnetic storms. *Journal of Atmospheric and Solar-Terrestrial Physics*, *67*(17-18), 1827–1836. doi: https://doi.org/10.1016/j.jastp.2005.07.004

Ngwira, C. M., Sibeck, D., Silveira, M. V., Georgiou, M., Weygand, J. M., Nishimura, Y., & Hampton, D. (2018). A study of intense local db/dt variations during two geomagnetic storms. *Space Weather*, *16*(6), 676–693. doi: https://doi.org/10.1029/2018SW001911

Parker, E. N. (1958). Dynamics of the interplanetary gas and magnetic fields. *The Astrophysical Journal*, *128*, 664.

Piddington, J. H. (1968, 06). The Causes and Uses of Geomagnetic Disturbance Index Kp. *Geophysical Journal International*, *15*(1-2), 39-52. doi: 10.1111/j.1365-246X.1968.tb05744.x

Pilipenko, V., Kozyreva, O., Belakhovsky, V., Engebretson, M., & Samsonov, S. (2010). Generation of magnetic and particle pc5 pulsations during the recovery phase of strong magnetic storms. *Proceedings of the Royal Society A: Mathematical, Physical and Engineering Sciences*, *466*(2123), 3363–3390. doi: https://doi.org/10.1098/rspa.2010.0079

Potapov, A., Guglielmi, A., Tsegmed, B., & Kultima, J. (2006). Global pc5 event during 29–31 october 2003 magnetic storm. *Advances in Space Research*, *38*(8), 1582 - 1586. (Magnetospheric dynamics and the international living with a star program) doi: https://doi.org/10.1016/j.asr.2006.05.010

Potapov, A., Tsegmed, B., & Polyushkina, T. (2009). Contribution of global pc5 oscillations to magnetic disturbance during geomagnetic storms. *Geomagnetism and Aeronomy*, *49*(8), 1182–1188. doi: https://doi.org/10.1134/S0016793209080295

Rae, I., Donovan, E., Mann, I., Fenrich, F., Watt, C. a., Milling, D., . . . others (2005). Evolution and characteristics of global pc5 ulf waves during a high solar wind speed interval. *Journal of Geophysical Research: Space Physics*, *110*(A12). doi: https://doi.org/10.1029/2005JA011007

Regi, M., De Lauretis, M., & Francia, P. (2015). Pc5 geomagnetic fluctuations in response to solar wind excitation and their relationship with relativistic electron fluxes in the outer radiation belt. *Earth, Planets and Space*, *67*(1), 1–9. doi: https://doi.org/10.1186/s40623-015-0180-8

Ridley, A., Lu, G., Clauer, C., & Papitashvili, V. (1998). A statistical study of the ionospheric convection response to changing interplanetary magnetic field conditions using the assimilative mapping of ionospheric electrodynamics technique. *Journal of Geophysical Research: Space Physics*, *103*(A3), 4023–4039. doi: https://doi.org/10.1029/97JA03328

Rolf, B. (1931). Giant micropulsations at abisko. *Terrestrial Magnetism and Atmospheric Electricity*, *36*(1), 9–14. doi: https://doi.org/10.1029/TE036i001p00009

Rostoker, G., Skone, S., & Baker, D. N. (1998). On the origin of relativistic electrons in the magnetosphere associated with some geomagnetic storms. *Geophysical Research Letters*, *25*(19), 3701–3704. doi: https://doi.org/10.1029/98GL02801

Samson, J., Jacobs, J., & Rostoker, G. (1971). Latitude-dependent characteristics of long-period geomagnetic micropulsations. *Journal of Geophysical Research*, *76*(16), 3675–3683. doi: https://doi.org/10.1029/JA076i016p03675

Southwood, D. (1968). The hydromagnetic stability of the magnetospheric boundary. *Planetary and Space Science*, *16*(5), 587–605. doi: https://doi.org/10.1016/0032-0633(68)90100-1

Southwood, D. (1976). A general approach to low-frequency instability in the ring current plasma. *Journal of Geophysical Research*, *81*(19), 3340–3348. doi: https://doi.org/10.1029/JA081i019p03340

Takahashi, K., & Ukhorskiy, A. Y. (2008). Timing analysis of the relationship between solar wind parameters and geosynchronous pc5 amplitude. *Journal of Geophysical Research: Space Physics*, *113*(A12). doi: https://doi.org/10.1029/2008JA013327

Torrence, C., & Compo, G. P. (1998, 01). A Practical Guide to Wavelet Analysis. *Bulletin of the American Meteorological Society*, *79*(1), 61-78. doi: 10.1175/1520-0477(1998)079⟨0061:APGTWA⟩2.0.CO;2

Tsurutani, B. T., Gonzalez, W. D., Tang, F., Akasofu, S. I., & Smith, E. J. (1988). Origin of interplanetary southward magnetic fields responsible for major magnetic storms near solar maximum (1978–1979). *Journal of Geophysical Research: Space Physics*, *93*(A8), 8519–8531. doi: https://doi.org/10.1029/JA093iA08p08519

Tsurutani, B. T., Gould, T., Goldstein, B. E., Gonzalez, W. D., & Sugiura, M. (1990). Interplanetary alfvén waves and auroral (substorm) activity: Imp 8. *Journal of Geophysical Research: Space Physics*, *95*(A3), 2241-2252. doi: 10.1029/JA095iA03p02241

Usoro, A. E., et al. (2015). Some basic properties of cross-correlation functions of n-dimensional vector time series. *Journal of Statistical and Econometric Methods*, *4*(1), 63–71.

Wang, B., Nishimura, Y., Hartinger, M., Sivadas, N., Lyons, L. L., Varney, R. H., & Angelopoulos, V. (2020). Ionospheric modulation by storm time pc5 ulf pulsations and the structure detected by pfisr-themis conjunction. *Geophysical Research Letters*, *47*(16), e2020GL089060. (e2020GL089060 2020GL089060) doi: 10.1029/2020GL089060

Wilcox, J. M. (1968). The interplanetary magnetic field. solar origin and terrestrial effects. *Space Science Reviews*, *8*(2), 258–328. doi: https://doi.org/10.1007/BF00227565

Wolfe, A., Lanzerotti, L., & Maclennan, C. (1980). Dependence of hydromagnetic energy spectra on solar wind velocity and interplanetary magnetic field direction. *Journal of Geophysical Research: Space Physics*, *85*(A1), 114-118. doi: https://doi.org/10.1029/JA085iA01p00114

Yamakawa, T., Seki, K., Amano, T., Takahashi, N., & Miyoshi, Y. (2019). Excitation of storm time pc5 ulf waves by ring current ions based on the drift-kinetic simulation. *Geophysical Research Letters*, *46*(4), 1911-1918. doi: https://doi.org/10.1029/2018GL081573